Capillarity

Vol. 18, No. 3, p. 83-95, 2026

Original article

Interfacial stability and bioactive potential of sustainable peppermint oil-mediated fluorescent selenium nanoparticles

Rawah Radhwan Abdulbari[1], Wasan M. Alwan[1], Rawaa H. Salman[2], Lekaa K. Abdul Karem[1], Ahmed A. El-Sayed[3], Ahmed M. Khalil[3]*

[1]*Department of Chemistry, College of Education for Pure Sciences (Ibn Al-Haitham), University of Baghdad, Baghdad 10053, Iraq*

[2]*Ministry of Education Iraqi Directorate of Education Baghdad Karkh III, Baghdad 10053, Iraq*

[3]*Photochemistry Department, National Research Centre, Giza 12622, Egypt*

Keywords:
Peppermint oil
selenium nanoparticles
colloid
antibacterial activity
fluorescence
interfacial behavior

Cited as:
Abdulbari, R. R., Alwan, W. M., Salman, R. H., Abdul Karem, L. K., El-Sayed, A. A., Khalil, A. M. Interfacial stability and bioactive potential of sustainable peppermint oil-mediated fluorescent selenium nanoparticles. Capillarity, 2026, 18(3): 83-95.
https://doi.org/10.46690/capi.2026.03.01

Abstract:
Synthesizing nanoparticles through green processes is a well-recognized challenge. It is a low-cost approach to produce multifunctional nanomaterials by using plant-based extracts as natural reductants and stabilizers. In this work, selenium nanoparticles were synthesized in Mentha piperita L. peppermint 3% as the concentration of the precursor solution. It is an essential oil containing bioactive compounds such as menthol, menthone, and flavonoids. The functionalized colloid of oil after being loaded with selenium nanoparticles is believed to exhibit enhanced properties. Fourier-transform infrared spectroscopy, ultraviolet-visible spectroscopy, and transmission electron microscopy have been employed to characterize the synthesized selenium nanoparticles. It was found that the selenium nanoparticles were uniformly distributed, spherical, and stable. Contact angle measurements showed that the selenium nanoparticles-loaded peppermint oil exhibited reduced hydrophobicity compared to pure oil, suggesting stronger interactions with polar surfaces. Interfacial interaction proposes that selenium nanoparticles preferentially migrate to the oil-water interface, reducing interfacial tension and stabilizing the colloidal system. This behavior contributes to the overall stability and uniformity of the oil/selenium nanoparticles conjugate. The present colloid displayed a significant enhancement in fluorescence. This confirms successful conjugation and enhanced optical performance, indicating their potential for bioimaging applications. Biological assessments demonstrated that the synthesized selenium nanoparticles and peppermint oil formulations exhibited significant antimicrobial and antioxidant properties. Hence, introducing these nanoparticles to peppermint oil increased its antioxidant capacity. The engineered colloidal system yielded a stable, fluorescent, and biologically active oil that may contribute to potential applications in bioimaging, antimicrobial therapy, antioxidant formulations, and nanotheranostics.

1. Introduction

Medicinal plants have been recognized as important sources of bioactive compounds for both traditional and modern medicine. Peppermint (Mentha piperita L.) has garnered considerable attention due to its diverse medicinal properties. It is widely applied in pharmaceutical, cosmetic, and food manufacturing (Yarnell, 2018). Mentha piperita L. is a fragrant perennial herb from the Lamiaceae family. It is a natural hybrid of Mentha aquatica and Mentha spicata. This plant

Yandy Scientific Press

*Corresponding author.
E-mail address: rawaa.r@ihcoedu.uobaghdad.edu.iq (R. R. Abdulbari); wasan.m.a@ihcoedu.uobaghdad.edu.iq (W. M. Alwan); rawaa.hajo2205@ihcoedu.uobaghdad.edu.iq (R. H. Salman); likaa.k.a@ihcoedu.uobaghdad.edu.iq (L. K. Abdul Karem).

Received November 29, 2025; revised December 26, 2025; accepted January 17, 2026; available online January 21, 2026.

grows in Africa, Europe, Asia, and North America (Zaidi and Dahiya, 2015). Ayurveda and other traditional systems of medicine have employed peppermint for hundreds of years (Aparna et al., 2017). Plant essential oils and phytochemicals, including phenolic acids, flavonoids (such as hesperidin and luteolin derivatives), tannins, terpenoids, and fatty acids, are all found in the plant's aerial portions (Bhuvaneshwari et al., 2007; Aparna et al., 2017). Peppermint oil is extracted as an essential oil from peppermint leaves. Menthol and menthone are the principal bioactive compounds among the volatile ones. This oil is able to heal infections, reduce inflammation, with advantageous analgesic properties (Park et al., 2012). The phytochemical study of peppermint essential oils from several global regions reveals considerable compositional heterogeneity. The oils' strength and ability to treat may be affected. A study of PEO from two different locations in Morocco, for example, indicated that the Azrou sample had a higher carvone content (70.25%). The Ouazzane sample had more menthol (43.32%) and menthone (29.4%) (Al-Mijalli et al., 2022a). This chemotypic diversity reveals how crucial the place and environment are in determining how well essential oils perform as medicines. There is extensive research on the impact of peppermint oil on living organisms. It operates as an antioxidant by getting rid of free radicals, decreasing oxidative stress, and stopping lipid peroxidation (Bhuvaneshwari et al., 2007). It lowers inflammation by stopping the action of pro-inflammatory cytokines (TNF-α and IL-6) and enzymes (lipoxygenase and cyclooxygenase). Some in vitro and in vivo investigations show that two PEOs can kill bacteria and fungi, especially Gram-positive bacteria (Yarnell, 2018; Al-Mijalli et al., 2022b). It is well-established that peppermint can help with digestive problems like irritable bowel syndrome. Moreover, it can help with respiratory infections, protect the liver and kidneys, and control metabolism (for example, by lowering blood sugar and cholesterol levels). Peppermint may alleviate some skin disorders like psoriasis and burns (Turner et al., 2000; Park et al., 2012). It is interesting to estimate the capability of peppermint oil to resist infections. PEO may cease the SARS-CoV-2 spike protein from attaching to the angiotensin-converting enzyme 2 receptor, which could stop the virus from getting into cells and the enzymes that help it to replicate (Aparna et al., 2017). Mentha piperita is a fascinating candidate for future pharmacological research and commercialization due to its varied chemical composition, extensive range of bioactivities, and longstanding history of therapeutic application.

Metallic nanoparticles exhibit antimicrobial, antiproliferative, and antioxidant activities. They possess unique physicochemical properties, which differ from their precursors. Their high surface area enhances interactions with microbial membranes, enabling effective inhibition of bacterial and fungal growth. In biomedical research, various metallic nanoparticles also exhibit antiproliferative effects by inducing oxidative stress, disrupting cellular signaling, or triggering apoptosis in cancerous cells. Additionally, their ability to scavenge free radicals supports strong antioxidant potential, making them valuable in therapeutic, pharmaceutical, and diagnostic applications (Abdelhamid et al., 2023; Tharp et al., 2024; Tharp et al., 2025). Peppermint (PM) is enriched with flavonoids as well as terpenoids. It allows nanoparticles to be more biologically active (Mahendran and Rahman, 2020; Jariani et al., 2024). This oil, renowned for its refreshing aroma and therapeutic properties, can be significantly enhanced when combined with selenium nanoparticles (SeNPs) (Dorman et al., 2009; Chakraborty et al., 2022). The synthesized SeNPs were probed to investigate their structural organization, morphology, and optical properties.. It is interesting to investigate their fluorescence as it showed how they interacted with each other and with the peppermint oil ingredients, particularly when combined with PM oil. Then, these nanoparticles produce a considerable amount of fluorescence. Mechanistically, this behavior demonstrates the construction of a stable hybrid nanostructure with improved optical properties that is appropriate for bioimaging. High antioxidant qualities and considerable antibacterial activity towards Candida albicans and both bacteria are among the remarkable biological activities displayed by the synthesized SeNPs. Subsequently, this innovative formulation leverages the antioxidant and antimicrobial potential of selenium at the nanoscale, which can improve the bioavailability and stability of the essential oil. The interfacial behavior between SeNPs and peppermint oil is governed by the distinct polarity and surface chemistry of each component. These synthesized nanoparticles via green methods typically possess surface-bound phytochemicals with polar functional groups, while peppermint oil is a predominantly nonpolar medium rich in hydrophobic constituents such as menthol and menthone. When SeNPs are introduced into the oil, their surface functionalities promote partial affinity for the oil phase while still retaining interfacial activity. As a result, the nanoparticles tend to migrate toward and stabilize the oil-water interface, where they reduce interfacial tension and enhance the colloidal stability of the system. This interfacial localization facilitates improved dispersion of the nanoparticles within the oil and supports the formation of a stable oil/SeNPs colloid. Increased hydrophobicity enhances Pickering emulsion stability by promoting nanoparticle adsorption at the oil-water interface. Simultaneously, it partially modifies the mineral surface wettability, allowing oil retention while maintaining sufficient water affinity to avoid complete oil-wet conditions. This combination enhances the stability and controllability of nanoparticle-oil conjugates in porous media. The modified interfacial environment also influences wetting behavior, often reflected in a slightly increased hydrophobicity relative to bare SeNPs. Commonly, these interfacial interactions contribute to the enhanced physicochemical and functional properties observed in peppermint oil loaded with SeNPs. Beyond its therapeutic potential, the physical chemistry of this oil-nanoparticle system provides a unique model for studying interfacial dynamics in porous media. Although CO_2-brine and SeNPs-peppermint oil systems involve different fluids, the underlying interfacial physics modulation of capillary forces, wettability, and pore-scale interface dynamics are conserved. The CO_2-brine literature thus provides a mechanistic foundation for understanding how capillary instabilities and interfacial evolution can influence nanoparticle-mediated phase behavior in porous media (Lv et al., 2024; Chang et al., 2025).

These are analogues for understanding capillary-driven transport and pore-scale displacement. Microfluidic experiments demonstrated how unsaturated CO_2 bubble morphology and interface evolution during drainage-imbibition cycles are governed by capillary forces and non-uniform dissolution (Lv et al., 2020; Xue et al., 2025). Complementary pore-scale simulations displayed that wettability heterogeneity across scales can control displacement pathways and trapping mechanisms. These findings may relate to our current work as microfluidic and pore-scale results on bubble morphology, snap-off, and mass transfer inform how nanoparticles can enhance oil mobilization by reshaping interfacial tension, promoting emulsion formation, and improving sweep efficiency in complex pore networks. The amphiphilic nature and surface chemistry of peppermint oil, featuring both hydrophobic terpenes and polar functional groups, enable strong adsorption onto nanoparticles, stabilize Pickering emulsions, and reduce interfacial tension. This feature makes it ideal for nanoparticle conjugation and interface-controlled formulations. Recent studies emphasize the role of nanoparticles in controlling interfacial phenomena and capillary-driven transport in porous media. Nanoparticle-modified gels and hybrid nanofluids have been shown to alter wettability and reduce interfacial tension, directly affecting capillary imbibition and droplet stability (Goharzadeh et al., 2023; Minakov et al., 2024). Studies of water-oil emulsions in porous systems provide additional insights into the interfacial mechanics relevant for nanoparticle-stabilized oil phases (Zarin et al., 2024).

Previous reports have described the plant-mediated synthesis of SeNPs (Mikhailova, 2023; Karthik et al., 2024) and the development of essential-oil-based nanocomposites (Guidotti-Takeuchi et al., 2022; Soni et al., 2023). Our work uniquely combines these two approaches by synthesizing SeNPs using peppermint oil and incorporating them into an essential-oil-based nanocomposite. This integrated strategy not only enhances the biocompatibility and stability of SeNPs but also introduces synergistic antimicrobial and antioxidant properties that have not been systematically explored in prior studies. Thus, our study provides a novel framework for the design of multifunctional, plant-mediated nanocomposites. Moreover, the current study aims to achieve an efficient, cost-effective, and environmentally friendly synthesis of SeNPs embedded in peppermint oil as a natural stabilizing and reducing agent. The synergistic interaction between peppermint oil and SeNPs may offer augmented health benefits for this colloid, including enhanced antibacterial activity, free radical scavenging, and potential protective effects against oxidative stress. Nano-enhanced peppermint oil exhibits considerable potential in pharmaceutical, cosmetic, and functional food applications due to its natural efficacy and safety.

2. Materials and methods

2.1 Materials

The PM oil was sourced from peppermint cultivated in Egypt. The following chemicals were acquired from Sigma Aldrich: methanol, dimethyl sulfoxide (DMSO), 1,1-diphenyl-2-picrylhydrazil (DPPH), and selenious acid (H_2SeO_3). A general-purpose culture medium, nutritional agar (NA) is ideal for less finicky microorganisms or for setting long-term cultures. The ingredients with a pH of 7.4 $\pm$ 0.2 are as follows: 2 g/L yeast extract, 5 g/L peptone, 1.0 g/L meat extract, 5 g/L NaCl, and 15 g/L agar. Yeast extract (2 g/L), peptone (5 g/L), meat extract (1 g/L), and sodium chloride (5 g/L) make up the nutrition broth medium, which has a pH of 7.4 $\pm$ 0.2. Sterile conical flasks with a volume of 100 mL were used to contain these compounds. The Gram-negative bacteria were the evaluated pathogenic microbes. "Escherichia coli" (ATCC 25922) and "Helicobacter pylori" (ATCC 43526), as well as Gram-positive bacteria: "Bacillus cereus" (ATCC 6629) and "Staphylococcus aureus" (ATCC 6538). Additionally, the pathogenic fungus "Candida albicans" (ATCC 10231) was included.

2.2 Synthesis of SeNPs (SeNPs@PM)

A conical flask was filled with 3 mL of peppermint oil PM and 10 mL of DMSO. Selenious acid (0.128 g, 0.1 mmol) was dissolved in 90 mL of deionized water and agitated at 60 °C. After that, peppermint oil emulsion (3%) was used as the control concentration in the following investigations. PM oil added dropwise for 1 hour to create an *in situ* suspension of SeNPs. The hue of the fluid shifted to red, indicating the creation of SeNPs (Alkherb et al., 2024). The synthesis was repeated independently three times under identical experimental conditions, and consistent nanoparticle formation was observed in all batches, as confirmed by UV-Vis spectroscopy, transmission electron microscopy (TEM) and particle size analysis. The average yield of SeNPs was calculated based on the initial selenium precursor concentration and the recovered nanoparticle mass, showing good reproducibility with minimal variation.

2.3 Characterization techniques

By using UV-Vis spectroscopy, a Shimadzu spectrophotometer tracked the development of SeNPs in peppermint oil, where the UV-Vis spectra were tracked. The structure and functional group analysis of the tested samples were investigated by Fourier-transform infrared spectroscopy (FTIR) (Perkin-Elmer PC1600, USA). The runs were carried out in the range 400-4,000 cm^{-1}. The formed SeNPs were tracked with High-Resolution TEM (HR-TEM) "JEOL" (JEM-2100). The suspension solution was sonicated, then applied to a 400-mesh "carbon-coated copper grid" to prepare the TEM samples. Contact Angle Tester (Hunan Gonoava Instrument Co., China) was employed to carry out contact angle investigations. All measurements were performed using the sessile drop method at room temperature (25 °C) for oil droplets with a volume of $\sim$ 5 µL, carefully deposited on a glass slide using a micro-syringe. The recorded values represent the average of 5 independent measurements taken for every sample. Perkin-Elmer (P. E.) LS 55 spectrophotometer was utilized to measure fluorescence spectra at low temperatures. It comprises an insulated chamber containing liquid N_2. The tests were carried out in a circular cuvette approximately 1 mm in diameter.

2.4 Antimicrobial efficiency

For determining the antibacterial activity of the prior samples, some experiments were conducted utilizing different human diseases; including gram-negative Staphylococcus aureus, Bacillus cereus, Helicobacter pylori, and Escherichia coli. Candida albicans is one type of Gram-positive fungus that was utilized in this study. Based on a previous technique (Osman et al., 2015), infectious strains were cultured in nutritious broth using fresh stocks, then incubated overnight. A separate strain of microbe was injected into each plate that contained 25.0 μL of the sterile nutrient agar medium (NA) (Hafez et al., 2023). A 0.6 cm cork borer was employed, and 75.0 μL of the previous samples were added to a 0.6 cm deep well using the well diffusion method (El-Masry et al., 2023). The inhibition zones were measured in millimeters. Chilling the plates is recommended to facilitate sample diffusion (Nalawade et al., 2016). The second group evaluated the bacteria's antimicrobial activity by colony forming unit (CFU) technique. In order to do this, tiny conical flasks were inoculated with bacterial suspensions (25.0 μL total volume) with nutritional broth medium (0.5 McFarland standard, 1.5×10^8 CFU/mL). Along with the infected flasks, 100 μL of the material that was examined was also added. The flasks were incubated at 37 °C (Purushothaman, 2018). For each strain, a sample-culture combination and a control flask have been serially diluted (10^{-1}-10^{-4}). The petri-dishes holding solidified nutritional agar were inoculated with 100.0 μL of the 10^{-4} dilution of the investigated samples each to find the microbial inhibition. Then, the following equation computed the reduction in growth rate R (%) for the treated samples against the control (untreated) samples:

$$R = \left(\frac{A-B}{A}\right) \times 100\% \quad (1)$$

where A represents CFU determined in the untreated control sample denoting pathogenic strains only without any treatment, mL; and B denotes viable counts determined in the tested treated sample.

The samples of peppermint (3%) and peppermint oil/SeNPs were subjected to another test for determining minimum inhibitory concentration (MIC) using nutrient broth medium through applying the broth microdilution method (Raoof et al., 2025). This method took place using microtiter enzyme-linked immunosorbent assay plates. In this process, each well of the plates was filled with 100.0 μL of nutrient broth medium, then by serial dilution technique, each sample was used separately in the first well by using the starting volume 100 μL; (50.0 mg/mL) of the used sample as a starting concentration. This is followed by transferring 100 μL from the first well to the second well, then transferring 100 μL from the second to the third, and so on to reach the final well that has a sample concentration of 390 μg of the used sample. Afterwards, the wells were inoculated with the tested pathogenic strains separately by transferring 100 μL (0.5 McFarland standard (1.5×10^8 CFU/mL)) of the tested strains. Finally, each well contained a final volume of 200 μL, and then the plates were incubated at 37 °C for 24 h. After the incubation period, the MIC was measured by reading the absorption of the inoculated plates using an enzyme-linked immunosorbent assay reader, where the mixture was shaken vigorously for 20 s and allowed to stand. The absorbance was then measured at 600 nm using a microplate multi-well reader (Bio-Rad Laboratories Inc., model 3350, Hercules, California, USA). The lower absorbance of the reaction mixture, equivalent to the absorption of the blank sample, is referred to as MIC activity.

2.5 Antioxidant activity

The free radical scavenging activity of the samples was assessed using 1,1-diphenyl-2-picrylhydrazyl ($DPPH^{\cdot}$), by following this procedure (Badawy et al., 2019). The volume (100 μL) was used to screen all of the samples. To summarize, $DPPH^{\cdot}$ was dissolved in 0.1 mM methanol. Afterwards, the previous sample was supplemented with 300 μL of the 0.1 mM DPPH solution. Every sample was tested thrice. After a vigorous shaking, the mixture was kept at 25 °C for 30 min. In a microplate reader, the absorbance was recorded. A lower absorbance value for the reaction mixture suggested that it was more effective in scavenging free radicals (El-Masry et al., 2023) was estimated through the inhibition % (I) as follows:

$$I = \left(\frac{A_0 - A_1}{A_0}\right) \times 100\% \quad (2)$$

where A_0 was the absorbance of the control reaction, and A_1 was the absorbance in the presence of the sample.

3. Results and discussion

3.1 Phytosynthesized selenium nanoparticles (SeNPs@PM)

The presence of numerous distinct components is confirmed by analyzing the phytochemicals of peppermint extract. Several of the bioactive phytochemicals included in PM have important physiological functions and have chemical structures that have been extensively studied and validated. According to reports, the IUPAC names of some of these components are included in the list (Aparna et al., 2017; Chakraborty et al., 2022). Hesperidin (3', 5, 7-trihydroxy-4'-methoxyflavanone 7-rutinoside), kaempferol, naringenin, quercetin, rutin, naringenin-7-O-glucoside, and hydroalcoholic extracts of Mentha piperita include flavonoids from several families; luteolin (3', 4', 5, 7-tetrahydroxyflavone); luteolin-7-O-glucoside; eriocitrin ((S)-3', 4', 5, 7-tetrahydroxyflavanone-7-[6-O-(α-L-rhamnopyranosyl)-β-D-glucopyranoside]), apigenin, etc.) (Dorman et al., 2009; Mahendran and Rahman, 2020; Aliki et al., 2021; Eftekhari et al., 2021); and phenolic acids, including caffeic acid and rosmarinic acid (Dorman et al., 2009; Aliki et al., 2021). The solvent used for extraction is the primary determinant of their concentrations in the final product. As seen in Fig. 1, the primary flavonoids found in Mentha piperita are chemically structured. In order to synthesize SeNPs and maintain their stability, the Se^+ cation was transformed to Se^0 utilizing hydroxyl groups. They served as oxygen sources. To decrease the concentration of Se^+ ions, organic compounds can employ reductive functional groups like −OH, −SH, and −NH. An obvious color change

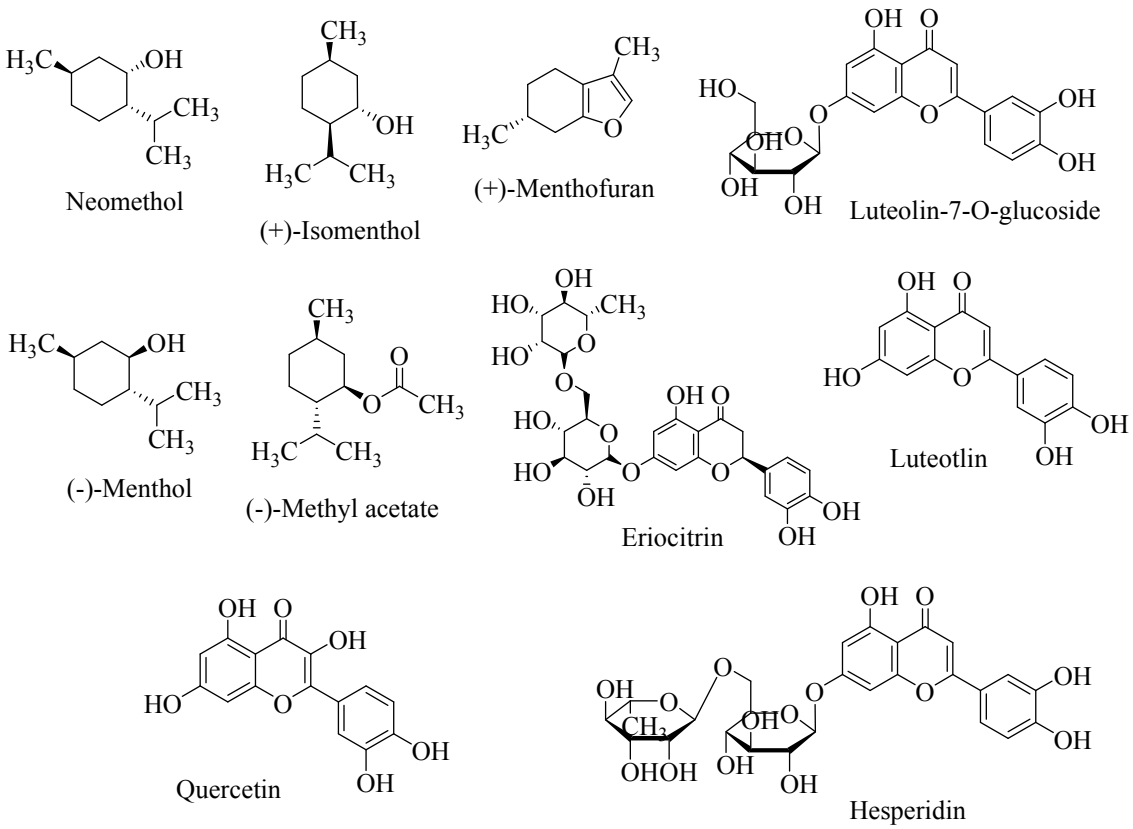

Fig. 1. Major chemical constituents of peppermint.

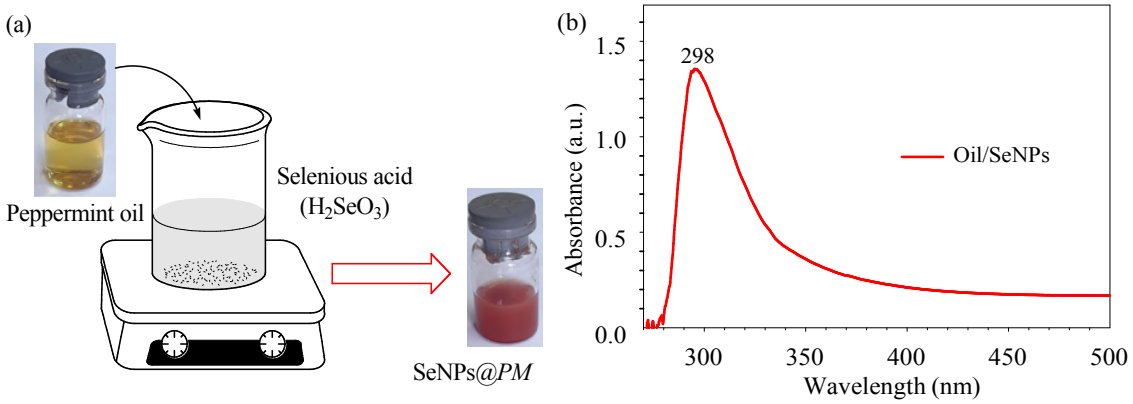

Fig. 2. A schematic diagram for synthesizing (a) SeNPs@PM and (b) UV-Vis spectrum of SeNPs@PM.

occurred during the production of SeNPs, which were created by reacting a Se^{+} salt with peppermint (Mentha piperita) essential oil.

3.2 Nanoparticles synthesis and characterization

A schematic diagram for the preparation process of SeNPs@PM is displayed in Fig. 2(a). The peppermint oil (3%), which was yellow before adding selenium salt, became a deep crimson color after being heated to about 60 °C overnight. UV-VIS spectroscopy was employed to assess the synthesis of SeNPs@PM. Our earlier work demonstrated that the synthesized SeNPs exhibit a broad absorption feature in the visible region (~ 450-520 nm), a characteristic reflecting nanoparticle nucleation and growth (Abdelhamid et al., 2023). It refers to the presence of surface plasmon resonance peaks for the formed nanoparticles. Because they didn't seem to aggregate, this feature indicates that the nanoparticles were formed and dispersed uniformly (Dahl et al., 2007; Soundarya et al., 2025). Upon encapsulation within the oil nanoemulsion, a pronounced absorption band appears in the UV region (~298 nm), indicating changes in the local dielectric environment and surface chemistry of SeNPs, which further supports the successful nanoformulation as shown in Fig. 2(b). Notably, the broadening and gradual decay of absorbance intensity suggest particle growth and stabilization processes occurring during the synthesis process.

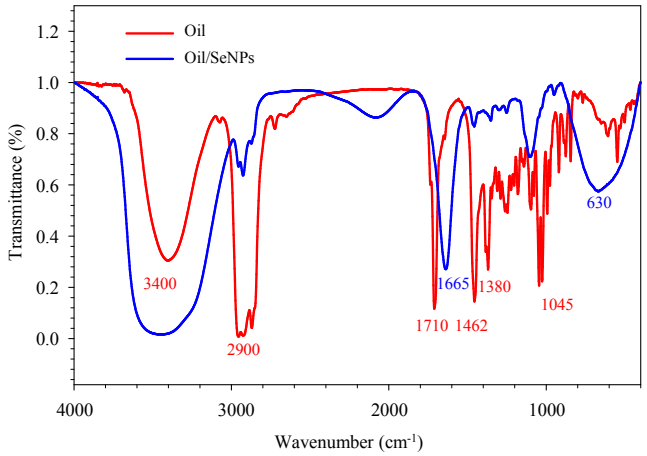

Fig. 3. FTIR spectra of oil and oil/SeNPs.

3.3 FTIR analysis of PM oil and SeNPs@PM

The FTIR spectra of the peppermint oil and the oil/SeNPs showed some differences, confirming the interaction of oil constituents with the selenium nanoparticle surface, as plotted in Fig. 3. For the oil spectrum; it showed a characteristic broad band absorption broad band. For the O−H group, a stretching band arose at 3,300-3,400 cm^{-1}, which is attributed to hydroxyl-containing terpene compounds such as menthol and menthone (Hashempur et al., 2025). On the other hand, C−H stretching peaks of aliphatic groups appear at 2,810-2,900 cm^{-1}, which are typical of methyl and methylene in essential oil components. The sharp peak at 1,710 cm^{-1} corresponds to C=O stretching of esterified and oxidized constituents, while the complex absorption patterns between 900-1,200 cm^{-1} represent C−O and C−H bending modes associated with terpenoids and oxygenated phytochemicals (Asbahani et al., 2015; Kamel et al., 2024). The FTIR spectrum for oil/SeNPs illustrated remarkable peak shifts and changes in intensity, indicating effective surface functionalization of SeNPs by PM oil constituents. The O−H stretching band broadened and slightly shifted, suggesting hydrogen bonding and coordination between hydroxyl groups and the nanoparticle surface (Das and Paul, 2025). Specifically, the broad O−H stretching vibration, centered at approximately 3,400 cm^{-1} in the pristine oil sample, becomes wider and more intense in the oil/SeNPs spectrum, indicating stronger hydrogen bonding interactions following nanoparticle incorporation. The C−H stretching vibrations at around 2,900 cm^{-1} remain present in both spectra, confirming the preservation of the oil's aliphatic structure. Furthermore, the aliphatic C−H stretching band exhibited reduced intensity, which is consistent with nanoscale surface adsorption of hydrocarbon bonds (Peng et al., 2021). The carbonyl peak also showed an outstanding shift from ∼1,710 to ∼1,665 cm^{-1}, indicating potential interaction of C=O groups with SeNPs, possibly through changes in local polarity during nanoparticle capping (Zhang et al., 2016). Notably, the carbonyl (C=O) stretching band shows a clear downshift in the oil/SeNPs sample. This shift of approximately 45 cm^{-1} suggests coordination or strong intermolecular interactions between the oil functional groups and the surface of SeNPs. A bending CH_2 peak arises at 1,462 cm^{-1} with asymmetric bending for the CH_3 group at 1,380 cm^{-1}, denoting the aliphatic chains of the oil. The C−O group of ester linkages and alcohol groups in the oil shows a peak at 1,045 cm^{-1}. Some variations in the intensity of peaks appear to indicate a possible interaction of the peppermint oil with the SeNPs surface. Changes in the fingerprint region were even clearer. The peaks attributed to C−O stretching and $-CH_2$ bending (1,000-1,200 cm^{-1}) decreased in intensity or shifted, suggesting strong involvement of ether, ester, and alcohol functional groups in stabilizing the nanoparticles. The band at 630 cm^{-1} represents the stretching and bending vibrations of Se−O. It can be referred to the binding of SeNPs to C=O groups resulting from oxidizing −COOH or −OH groups. Hence, they surround SeNPs, avoiding agglomeration. Similar metal nanoparticle systems in essential oil modifications have been consistently reported and referred to as phytochemical-mediated reduction and coated nanoparticles (Abdel-Raouf et al., 2017; Shahzadi et al., 2025). Relative intensity changes were evaluated by comparing these spectra, revealing an increase in the O−H band intensity and a reduction in carbonyl peak sharpness after SeNPs incorporation. IR spectral shifts confirm the successful binding of PM oil constituents, particularly hydroxyl, carbonyl, and ether functional groups, to the surface of the selenium nanoparticle. Such interaction likely enhances nanoparticle stability, biocompatibility, and biological activity, which is critical for potential vector-control applications. These observations cope with earlier investigations in the literature. They demonstrate that plant-derived secondary metabolites act essentially to synthesize and stabilize metal and metalloid nanoparticles (Balaji et al., 2025).

The formation of SeNPs is depicted in Fig. 4. It was confirmed by the TEM analysis. This technique elucidates the composition of the prepared SeNPs, as shown in Fig. 4(a). Spherical particles are noticed, with a high level of uniformity. They express the diffusion of these nanoparticles in the oil matrix. Well-dispersed, stable particles may be correlated with the capping effect of the oil that embeds these nanoparticles. This form for poly-dispersed nanoparticles extends the efficiency of these nanoparticles with an anisotropic behavior. Thereafter, an enhanced chemical influence for these SeNPs is expected. Selected area electron diffraction image in Fig. 4(b) detected an amorphous form for SeNPs@PM. The absence of crystallinity of these nanoparticles can be correlated to the abundance of the adhering oil around the synthesized nanoparticles. The zeta potential of SeNPs in peppermint oil is a key parameter reflecting their surface charge and colloidal stability. High absolute zeta potential values indicate strong electrostatic repulsion among nanoparticles, minimizing aggregation and contributing to enhanced dispersion stability, functional performance, and shelf-life of the oil-capped SeNPs. Fig. 4(c) shows zeta potential at (-28 ± 6.73 mV). The findings showed that the produced SeNPs had a narrow size range. Featuring a spherical morphology with a typical particle size ranging from 9 to 14 nm, SeNPs were generated by this eco-friendly method with enduring stability, as displayed in Fig. 4(d).

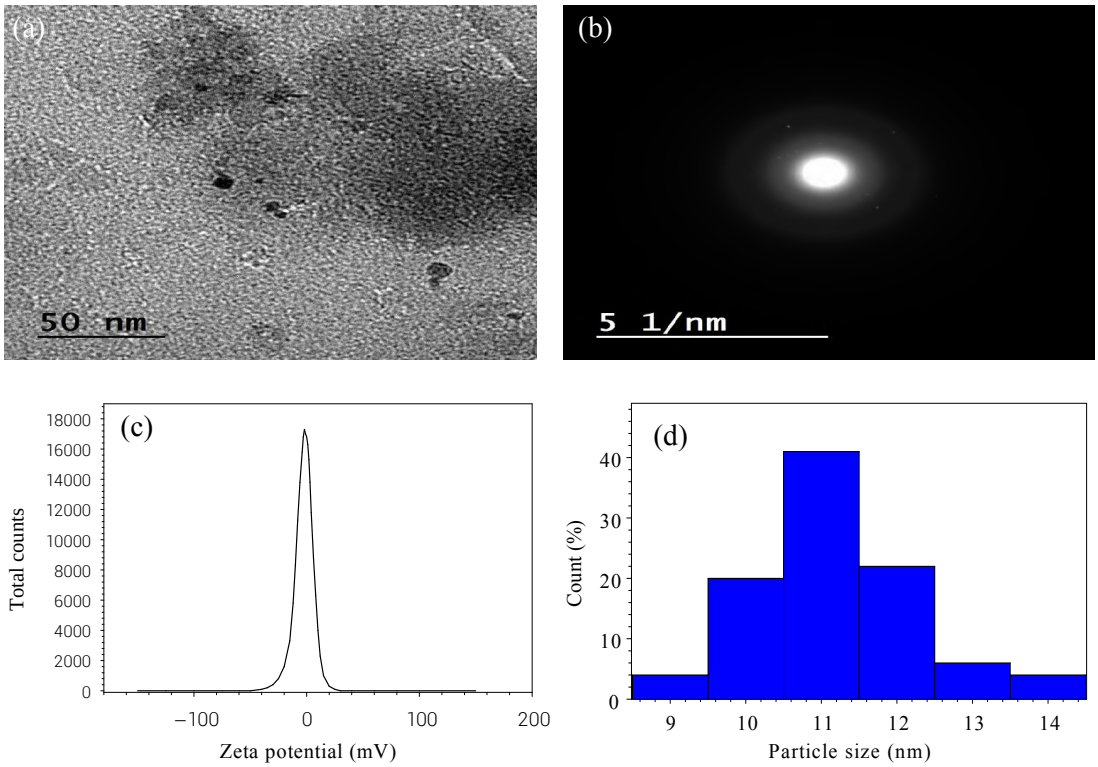

Fig. 4. Oil/SeNPs: (a) TEM image, (b) selected area electron diffraction, (c) zeta potential, and (d) particle size distribution.

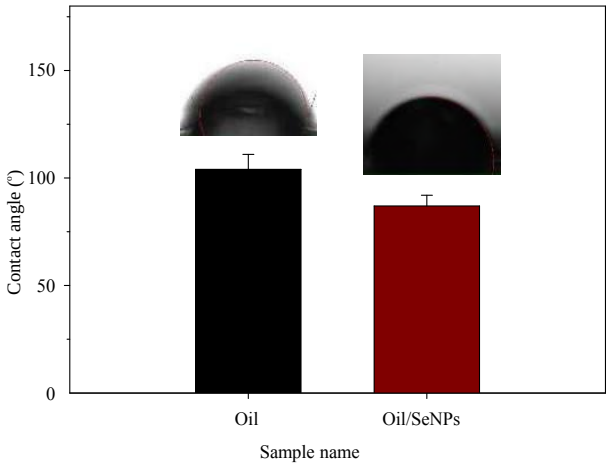

Fig. 5. Contact angle measurements of peppermint oil and the oil loaded with SeNPs.

3.4 Contact angle measurements

Contact angle investigations were conducted to assess the impact of loading peppermint oil with SeNPs on surface wettability and interfacial behavior. The tested samples were placed on glass slides as displayed in Fig. 5. For the peppermint oil sample, its contact angle was 104°. This behavior reflects the formation of a mildly hydrophobic organic film attributed to the essential oil components. This confirms the formation of a hydrophobic organic film associated with terpene-rich oil components. In contrast, the surface of oil/SeNPs exhibited a contact angle of 86°. The decrease in hydrophobicity can be correlated to pure peppermint oil. It is affected by the presence of SeNPs and polar phytochemical capping groups. Subsequently, it may increase surface energy by introducing nanoscale roughness. These wettability changes have direct implications for capillary spreading, interfacial adhesion, and liquid infiltration through porous structures. From a biomedical standpoint, the modified wettability may also influence microbial attachment and fluid distribution across treated surfaces, supporting the functional role of oil/SeNPs as bioactive and interfacially active colloids. Consequently, contact angle investigation controlled interfacial properties not only through governing capillary transport and liquid penetration but also augmented antimicrobial efficiency (as it will be discussed later), illustrating how interfacial engineering can synergistically enhance both physical and bioactive performance of nanoparticle coatings. It is estimated that the interfacial coverage of SeNPs using the reported particle size and concentration suggests that a significant fraction of SeNPs can adsorb at the interface, consistent with the observed stabilization of the emulsion. This supports their strong tendency to accumulate at the oil-water interface. The adsorption of SeNPs reduces the interfacial energy. Hence, this behavior becomes consistent with their tendency to accumulate at the interface and contribute to emulsion stabilization, providing quantitative support for the interpretation presented in this work. Relevant studies (Du et al., 2010; Huang and Keddie, 2025) revealed that nanoparticles at oil-water interfaces experience adsorption energy whose magnitude exceeds the thermal energy of particles < 100 nm in radius at ambient temperature 25 °C. Here, it is noticeable to explain that these SeNPs possess a strong tendency to oc-

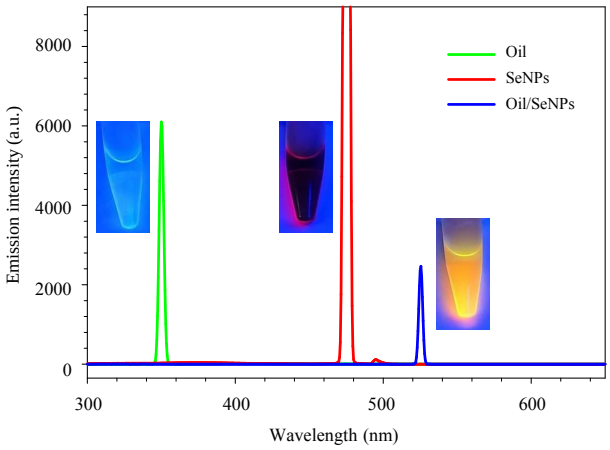

Fig. 6. Fluorescence emission spectra of peppermint oil, SeNPs, and their conjugate (oil/SeNPs).

cupy and stabilize the interface alike in Pickering emulsions. The contact angle values are now reported as mean values with standard deviation of 15.65 and 13.42 for oil and oil/SeNPs, respectively. It reflects the reproducibility of the measurements. As shown in Fig. 5, the incorporation of SeNPs leads to a statistically significant change in surface wettability compared to the pristine oil surface, confirming the successful modification of surface properties. SeNPs are liberated to the oil-water interface. Consequently, they minimize interfacial free energy, replacing high energy oil-water contact with lower energy particle-fluid contacts. This adsorption lowers interfacial tension. According to the Young-Laplace equation (Liu and Cao, 2016), it reduces capillary pressure, stabilizing droplets against coalescence and enhancing the persistence of nanoparticle-oil phases.

3.5 Fluorescence characteristics of SeNPs@PM

Under the same excitation conditions, the fluorescence spectra of peppermint oil-capped SeNPs (SeNPs@PM) alongside the oil and Se nanoparticles were captured as shown in Fig. 6. PM oil showed a single, strong near-UV emission band that was centered in the 350 nm range (Piacenza et al., 2020) in the visible spectrum with medium intensity (Maffei et al., 1999; Ghayempour and Montazer, 2017). Another strong peak arises referring to SeNPs, which appears at 482 nm. Furthermore, peppermint oil-capped SeNPs (SeNPs@PM) showed a third weak but wider band spanning at 524 nm, with intensity exceeding 10,000 a.u. SeNPs@PM's emission intensity rapidly decreased beyond 550 nm, suggesting that there was no discernible dark red fluorescence. The intense emission at about 335 nm is produced by Förster resonance energy transfer. The excited PM molecules act as donors and SeNPs as acceptors, made possible by the spectral overlap between PM absorption bands (near-UV) and SeNPs excitation (Lakowicz, 2006). The significant increase in UV fluorescence intensity following capping of SeNPs showed that the components of peppermint oil serve as stabilizing and capping agents with lowering surface traps on the nanoparticle and promoting effective radiative recombination. The PM oil comprises a content of menthone and menthol with some terpenes and phenolics. They are most likely adsorbed on the surface of SeNPs, allowing photoinduced energy transfer from excited oil molecules to SeNPs states (Tran and Webster, 2011; Karthik et al., 2024). When compared to PM alone, this energy transfer and surface dress together explaining the magnitude of increase in emission. The broad visible emission band in the SeNPs@PM spectrum, which is not present in the PM oil, could be the result of defect-related emissive centers stabilized by the organic moieties or ligand to nanoparticle charge-transfer states. This implies that the core of SeNPs and phytochemicals is surface-bound and interacts intricately to produce a variety of emissive pathways. SeNPs@PM are a good choice for bioimaging applications that need bright and stable UV-excited probes since they have strong UV emission and noticeable fluorescence. These nanohybrids are especially useful for fluorescence-based sensing in antimicrobial systems because they can monitor interactions between nanoparticles and biomolecules using optical readouts. The increased emission is a useful method for testing how stable and absorbent nanoparticles are in biological contexts. The comparison study shows that when SeNPs are added to peppermint oil, its natural fluorescence is enhanced and new emissive qualities are created. This behavior shows that SeNPs@PM could be useful for different environmental or medical applications.

Our results coincide with earlier studies that used components of essential oils as natural reductants and stabilizers during the formation of SeNPs. It was stated that energy transfer from eugenol enhanced the fluorescence of silver nanoparticles stabilized with clove oil (Gherasim et al., 2020). Similarly, research suggests that SeNPs stabilized by plant polyphenols have significant UV-blue fluorescence attributed to the formation of emissive defect states and a decrease in non-radiative losses (Avendaño et al., 2023; Zambonino et al., 2023). In contrast, research on uncapped or chemically stabilized SeNPs generally demonstrates reduced and broader emission patterns, highlighting the critical function of organic natural capping agents in fluorescence modulation. Furthermore, the photophysical behavior of ligand-nanoparticle charge-transfer complexes reported for thiol- and amine-functionalized SeNPs is similar to the appearance of a new visible emission in SeNPs@PM. These findings assume that peppermint oil both stabilizes the surface of the nanoparticle and actively modifies its electronic structure, generating new defect-mediated emissive states that improve and broaden the overall fluorescence response.

3.6 Antimicrobial efficiency

Among the considerable medical breakthroughs of the 20th century, it is worth mentioning the development of potent antibacterial drugs. Based on their site of activity, antimicrobial agents can inhibit cell wall synthesis, protein synthesis, nucleic acid synthesis, or disruption of cell membrane integrity. These four categories determine how antimicrobial agents work against pathogens that originate in plants, animals, or humans. In addition, there were primarily two types of antibacterial agents. Bactericidal agents, which may eliminate germs directly, are part of the first one. By this effect, the

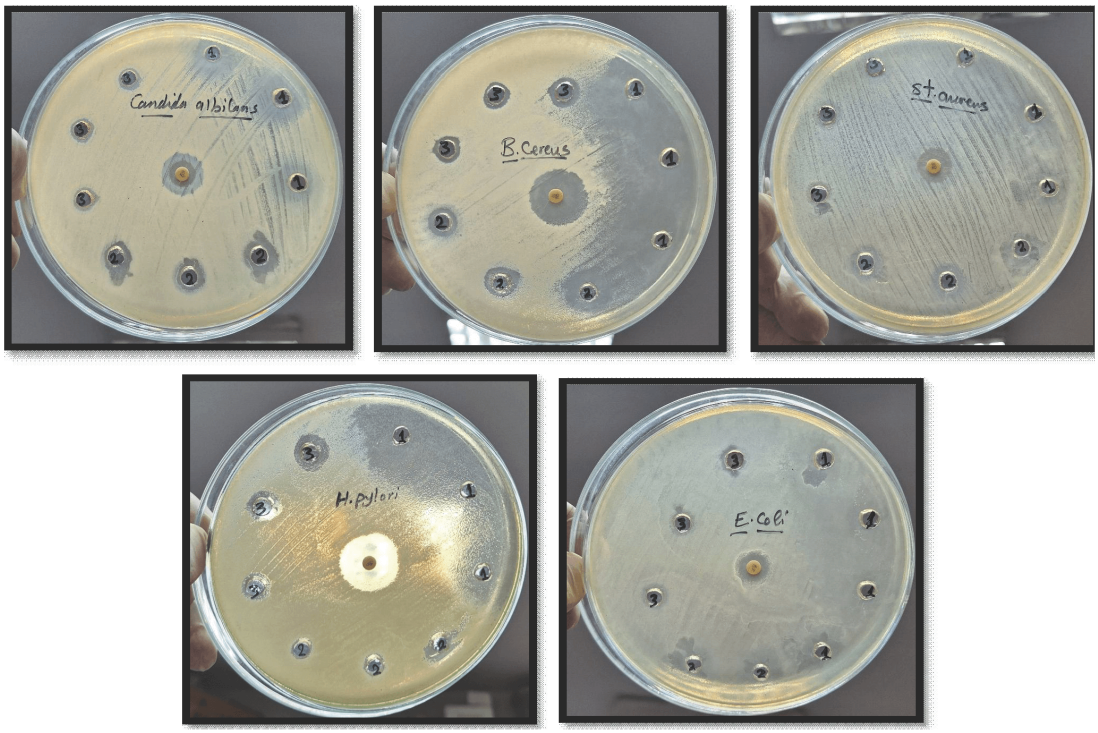

Fig. 7. Inhibition zone produced by peppermint oil, 3% oil, and oil/SeNPs.

Table 1. Inhibition zone diameter (millimeters) of the samples.

No.	Testing bacteria or fungi	Treated sample									
		Peppermint oil (crude)			Peppermint oil (3%)			Oil/SeNPs			Reference (CN)
1	Escherichia coli	12	12	13	12	11	13	11	12	12	17
2	Helicobacter pylori	30	33	31	15	13	12	16	16	7	22
3	Bacillus cereus	30	29	28	21	16	14	20	21	10	20
4	Staphylococcus aureus	15	15	16	15	12	14	15	13	3	22
5	Candida albicans	15	19	18	17	15	15	14	14	4	20

Notes: Reference (CN) represents gentamicin 10 mcg (standard antibiotic disc).

relative inoculum density during a certain incubation time up to 24 h decreases by a ratio of 99.9 percent. This feature results in a decrease the amount of viable colony-forming units of bacteria (Martini et al., 2024). Those antimicrobials that also have a bacteriostatic activity constitute the second group. This term refers to an agent that inhibits the growth or reproduction of bacteria without killing them. These agents are described as bacteriostatic agents (Balouiri et al., 2016). Using the well diffusion method, the substances listed in Table 1 exhibited remarkable antibacterial activity in this experiment. After testing the samples against both Gram-positive and Gram-negative bacteria, it was used to quantify the diameter of the inhibitory zone. Staphylococcus aureus and Bacillus cereus, and the Gram-negative bacteria Escherichia coli and Helicobacter pylori, in addition to the pathogenic yeast fungal strain Candida albicans. The following forms of peppermint oil were evaluated: undiluted, diluted to 3%, and SeNPs coated with 3% peppermint oil. The materials tested had an inhibitory zone ranging from 12 to 30 mm when tested against Gram-positive bacteria. With an inhibitory zone range of 11-33 mm, the identical samples demonstrated outstanding antibacterial efficacy against Gram-negative bacteria. In addition, the anti-fungal action of these earlier samples was demonstrated by an inhibition zone range of 14-19 mm against the fungus strain Candida albicans. The results in Fig. 7 were matched, and in some cases even surpassed previously reported findings (Al-Mijalli et al., 2022a). These samples effectively eradicated nearly all bacteria in the culture. The bacterial and fungal strains that are utilized can be killed, or their growth or reproduction can be entirely halted by these substances.

Therefore, the compounds that were examined show promise as agents that can destroy bacteria and fungi. These samples work by preventing the bacterial cell membrane from releasing its contents. The antibacterial activity and mechan-

Table 2. The MIC of the tested samples applying the broth microdilution method.

Testing bacteria or fungi	Sample concentration		
	Peppermint oil (3%) (mg/mL)	Oil/SeNPs (mg/mL)	Gentamicin (CN) (μg/mL)
Escherichia coli	37.5	17.5	94.0
Helicobacter pylori	18.75	17.5	125.0
Bacillus cereus	19.5	9.5	125.0
Staphylococcus aureus	19.5	9.5	118.0
Candida albicans	37.5	17.5	60.0

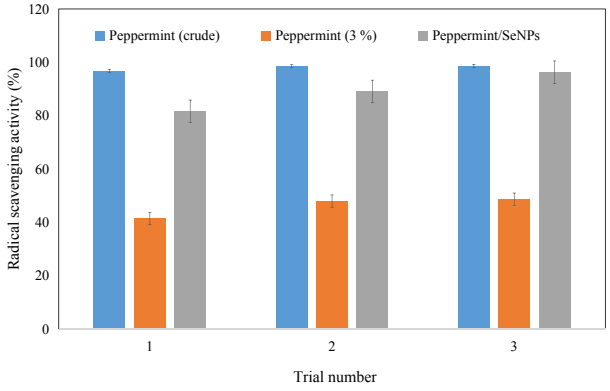

Fig. 8. Evaluation of peppermint oil (crude), oil (3%), and oil/SeNPs antioxidant properties.

ism of these materials, in conjunction with the produced nanoemulsions, thereby impact the cell walls of both bacteria and fungi. The samples' fusing ability with the test strains' outer membranes caused an electrostatic contact between the nanoparticles' cationic charge and the microbes' anionic charge, leading to these results (Hwang et al., 2013). In the end, disruption occurs as a result of lipid bilayer destabilization and cellular permeability (Pisoschi et al., 2018). When SeNPs are dispersed in peppermint oil, the surface tension of the mixture typically decreases compared to pure oil. This reduction occurs because nanoparticles tend to accumulate at the oil-water or oil-cell interface, altering interfacial behavior. Lower surface tension enhances the ability of the oil/SeNPs system to spread, wet, and interact with microbial cell membranes. Hence, several cascade events, such as suppression of nucleic acid production, are caused by the broad-spectrum activity of these samples, penetrating the bacteria. Enzyme inactivation, membrane rupture due to inhibition of ATPase activity, loss of vital biomolecules from the cell, disturbance of the natural and motive forces, and protein synthesis inhibition are the subsequent metabolic activities of bacteria that are inhibited. Additionally, essential oils of Mentha piperita were employed to suppress bacterial protein production by working throughout the attachment to and destruction of bacterial ribosomes. From the previous actions, the investigated samples showed an excellent antimicrobial result against the previously employed pathogenic strains. Finally, these samples have an excellent antimicrobial activity against Gram-positive bacteria, Staphylococcus aureus and Bacillus cereus alongside Gram-negative bacteria, Escherichia coli & Helicobacter pylori. They exhibit a potent antimicrobial effect, making them promising antimicrobial agents that can be used in various implementations. The latter ones comprise food packaging, healthcare, and drug-related domains, especially in surgical, burners, and wound healing tools.

The MICs of peppermint oil (3%), peppermint oil-SeNPs, alongside gentamicin against selected bacteria and Candida albicans are represented in Table 2. Entirely, the oil/SeNPs sample consistently shows lower MIC values than peppermint oil alone for all tested microorganisms. This behavior indicates enhanced antimicrobial efficacy after nanoparticle formulation. For example, Escherichia coli and Candida albicans exhibit MICs of 17.5 mg/mL with oil/SeNPs compared to 37.5 mg/mL with peppermint oil, while Bacillus cereus and Staphylococcus aureus show particularly low MICs of 9.5 mg/mL with Oil/SeNPs. In comparison, gentamicin displays much higher MIC values (60-125 μg/mL), especially against Helicobacter pylori, Bacillus cereus, and Staphylococcus aureus, which suggests lower effectiveness under the tested conditions. Collectively, these results indicate that peppermint oil, particularly when combined with SeNPs, demonstrates strong antimicrobial potential across both Gram-positive, Gram-negative bacteria and fungal strains.

3.7 Antioxidant activity

Diluted peppermint oil (3%) and SeNPs coated with 3% peppermint oil were assessed through a radical scavenging activity assay. Crude peppermint oil is an effective antioxidant, scavenging radicals at a mean percentage of 97.97%. It shows that there is a strong resistance against free radicals. The results were fairly consistent and could be repeated in later trials because the standard deviation was just 0.85 and the standard error was only 0.49. The average antioxidant activity of the 3% peppermint oil diluted solution, on the other hand, was just 45.96%. The quick decline is because bioactive compounds like menthol and flavonoids, which are known to promote antioxidant activity, are no longer present. Transforming 3% peppermint oil into SeNPs increased the antioxidant activity to 88.97%, as seen in Table 3 and Fig. 8, despite a decrease in oil quantity. It is quite likely that the synergistic effects of SeNPs are responsible for this enhancement. With the essential oil components, these nanoparticles are known for their inherent antioxidant properties. Additionally, the nanoparticle delivery technology's larger surface area and higher bioavailability may have made radical scavenging more effective. The SeNPs had a higher standard deviation (5.99) than the crude oil, which means that there was some variation. In general, the results show that nano-formulation can greatly restore and even boost the bioactivity of diluted natural extracts. These results suggest that SeNPs coated with peppermint oil are a viable approach to enhance antioxidant capacity in formulations with reduced

Table 3. Antioxidant activity of the investigated samples with radical scavenging activity (%).

Samples	Trials			Mean	Standard deviation	Standard error
	1	2	3			
Peppermint (crude)	96.77	98.51	98.63	97.97	0.85	0.4907
Peppermint (3%)	41.35	47.92	48.62	45.96	3.27	1.890
Peppermint/SeNPs	81.59	89.05	96.27	88.97	5.99	3.460

concentrations. Although the antioxidant effect arises from the intrinsic chemical properties of the colloidal peppermint oil and SeNPs system, reduced surface tension and engineered capillarity promote better dispersion and interfacial contact with reactive oxygen species. They indirectly enhance the measurable antioxidant activity.

4. Conclusions

The current work demonstrated a green production of coated SeNPs using mentha piperita L. (peppermint) oil as a natural reductant and stabilizer. The resulting oil was enhanced after loading SeNPs into it. These nanoparticles were spherical, uniformly dispersed, and demonstrated exceptional optical and biological properties. The peppermint oil-SeNPs colloid generated a stable hybrid nanostructure with promising optical properties suitable for bioimaging, as evidenced by fluorescence studies indicating substantial light emission. In contact angle measurements, peppermint oil loaded with SeNPs displayed lower hydrophobicity when compared to peppermint oil, implying a stronger affinity for nonpolar surfaces. Interfacial analysis further showed that the nanoparticles tended to migrate toward the oil-water interface, lowering interfacial tension and enhancing colloidal stability. This behavior plays a key role in maintaining the overall stability and homogeneity of the oil/SeNP conjugate. Naturally occurring SeNPs exhibit remarkable antibacterial efficacy against Candida albicans as well as Gram-positive and Gram-negative microorganisms. They demonstrated their ability to eradicate a variety of microorganisms. The inhibitory zones varied in size from 11 to 33 mm. The findings display a wide-ranging bactericidal and fungicidal effect owing to electrostatic forces acting between cationic SeNPs and anionic microbial membranes, leading to metabolic inhibition and membrane disruption. In addition, antioxidant tests showed that crude peppermint oil had a radical scavenging activity of 97.97%. Meanwhile, 3% diluted oil displayed a radical scavenging activity of 45.96%, and PM oil loaded with SeNPs showed 88.97%. This implies that the peppermint and selenium phytochemicals work together to make the oil more effective. The enhanced antioxidant activity of the peppermint oil/SeNPs colloid is affected by surface tension, as it improves spreading and interfacial contact, thereby facilitating more efficient interaction with reactive oxygen species. A green potent pathway is now ready to generate multifunctional nanoparticles able to destroy some germs and protect against free radicals via the synthesized SeNPs. Decreased surface tension allows the nano-oil system to spread more effectively across bacterial surfaces, increasing the likelihood of membrane disruption. Results show promise for the ameliorated peppermint oil/SeNPs in biomedicine, nanotheranostic systems, bioimaging, wound healing, and pharmacology. Further studies could focus on cytotoxicity studies, in vivo evaluations, and the optimization of nano-formulation parameters for specific biomedical applications.

Acknowledgements

This is an optional element, and offers the author(s) an opportunity to address supporters and/or contributors to the paper.

Additional information: Author's email

ahmedcheme4@yahoo.com (A. A. El-Sayed);
akhalil75@yahoo.com (A. M. Khalil).

Conflicts of interest

The authors declare no competing interest.

References

Abdelhamid, A. E., El-Sayed, A. A., Swelam, S. A., et al. Encapsulated polycaprolactone with triazole derivatives and selenium nanoparticles as anticancer agents. ADMET and DMPK, 2023, 11(4): 561-572.

Abdel-Raouf, N., Al-Enazi, N. M., Ibraheem, I. B. M. Green biosynthesis of gold nanoparticles using Galaxaura elongata and characterization of their antibacterial activity. Arabian Journal of Chemistry, 2017, 10: S3029-S3039.

Aliki, T., Archontoula, C., Evaggelos, Z., et al. Antioxidant activity of Mentha piperita L. of Greek flora. International Organic and Medicinal Chemistry Journal, 2021, 11(3): 555814.

Alkherb, W. A. H., Farag, S. M., Alotaibi, A. M., et al. Pyrazolopyrimidine derivatives conjugated with selenium nanoparticles for larvicidal activity. Colloids and Surfaces B: Biointerfaces, 2024, 241: 114040.

Al-Mijalli, S. H., Assaggaf, H., Qasem, A., et al. Antioxidant, antidiabetic, and antibacterial potentials and chemical composition of Salvia officinalis and Mentha suaveolens. Advances in Pharmacological and Pharmaceutical Sciences, 2022a, 2022(1): 2844880.

Al-Mijalli, S. H., Mrabti, N. N., Ouassou, H., et al. Phy-

tochemical variability and antibacterial mechanisms of Mentha piperita. Foods, 2022b, 11(21): 3466.

Aparna, L. M., Aparna, S., Sarada, I., et al. Assessment of sputum quality and its importance in the rapid diagnosis of pulmonary tuberculosis. Archives of Clinical Microbiology, 2017, 8(4): 53.

Asbahani, A. El, Miladi, K., Badri, W., et al. Essential oils: extraction to encapsulation. International Journal of Pharmaceutics, 2015, 483(1-2): 220-243.

Avendaño, R., Muñoz-Montero, S., Rojas-Gätjens, D., et al. Selenium nanoparticle production in Pseudomonas putida. Microbial Biotechnology, 2023, 16(5): 931-946.

Badawy, M. E. I., Lotfy, T. M. R., Shawir, S. M. S. Chitosan-silver nanoparticles for meat preservation. Bulletin of the National Research Centre, 2019, 43(1): 83.

Balaji, S., Pandian, M. S., Ganesamoorthy, R., et al. Green synthesis of metal oxide nanoparticles using plant extracts: A sustainable approach to combat antimicrobial resistance. Environmental Nanotechnology, Monitoring & Management, 2025, 23: 101066.

Balouiri, M., Sadiki, M., Ibnsouda, S. K. Methods for in vitro antimicrobial evaluation. Journal of Pharmaceutical Analysis, 2016, 6(2): 71-79.

Bhuvaneshwari, L., Arthy, E., Anitha, C., et al. Phytochemical analysis and antibacterial activity of Nerium oleander. Ancient Science of Life, 2007, 26(4): 24-28.

Chakraborty, K., Chakravarti, A. R., Bhattacharjee, S. Bioactive components of peppermint (Mentha piperita L.). Journal of Pharmacognosy and Phytochemistry, 2022, 11(1): 109-114.

Chang, Y., Xue, R., Wang, S., et al. Scale-dependent dynamics of CO_2-brine interfaces in mixed-wetting porous media: From sub-grain to grain levels. Physics of Fluids, 2025, 37(6): 0267616.

Dahl, J. A., Maddux, B. L. S., Hutchison, J. E. Toward greener nanosynthesis. Chemical Reviews, 2007, 107(6): 2228-2269.

Das, D., Paul, P. Environmental impact of silver nanoparticles and its sustainable mitigation by novel approach of green chemistry. Plant Nano Biology, 2025, 14: 100210.

Dorman, H. J. D., Koşar, M., Başer, K. H. C., et al. Phenolic profile and antioxidant evaluation of Mentha x piperita L. extracts. Natural Product Communications, 2009, 4(4): 535-542.

Du, K., Glogowski, E., Emrick, T., et al. Adsorption energy of nano-and microparticles at liquid-liquid interfaces. Langmuir, 2010, 26(15): 12518-12522.

Eftekhari, A., Khusro, A., Ahmadian, E., et al. Phytochemical and nutra-pharmaceutical attributes of Mentha spp.: A comprehensive review. Arabian Journal of Chemistry, 2021, 14(5): 103106.

El-Masry, H. M., Atwa, N. A., El-Beih, A. A., et al. Phenazine-producing Pseudomonas aeruginosa OQ158909: A promising candidate for biological activity and therapeutic applications. Egyptian Journal of Chemistry, 2023, 66(11): 281-303.

Ghayempour, S., Montazer, M. Herbal products on cellulosic fabric with controlled release: Comparison of *in situ* encapsulation and UV curing of the prepared nanocapsules. Cellulose, 2017, 24(9): 4033-4043.

Gherasim, O., Puiu, R. A., Bîrca, A. C., et al. An updated review on silver nanoparticles in biomedicine. Nanomaterials, 2020, 10(11): 2318.

Goharzadeh, A., Fatt, Y. Y., Sangwai, J. S. Effect of TiO_2-SiO_2 hybrid nanofluids on enhanced oil recovery process under different wettability conditions. Capillarity, 2023, 8(1): 1-10.

Guidotti-Takeuchi, M., Ribeiro, L. N. D. M., Dos Santos, F. A. L., et al. Essential oil-based nanoparticles as antimicrobial agents in the food industry. Microorganisms, 2022, 10(8): 1504.

Hafez, A. I., Ali, H. M., Sabry, R. M., et al. Hygienic and cost-effective nanostructured core-shell pigments. Progress in Organic Coatings, 2023, 175: 107325.

Hashempur, M. H., Ghorat, F., Karami, F., et al. Topical delivery systems for plant-derived antimicrobials. International Journal of Biomaterials, 2025, 2025: 4251091.

Huang, Z., Keddie, J. L. Free energy modelling of a spherical nanoparticle at an oil/water interface. Soft Matter, 2025, 21(26): 5188-5193.

Hwang, Y. Y., Ramalingam, K., Bienek, D. R., et al. Nanoemulsion with cetylpyridinium chloride against A. baumannii. Antimicrobial Agents and Chemotherapy, 2013, 57(8): 3568-3575.

Jariani, P., Sabokdast, M., Moghadam, T. K., et al. Modulation of phytochemical pathways and antioxidant activity in peppermint by salicylic acid and GR24. Cells, 2024, 13(16): 1360.

Kamel, O. M. H. M., El-halim, M. D. A., Khalil, A. M., et al. A promising route to control mosquito larvae by metal nanoparticles. Egyptian Journal of Aquatic Biology and Fisheries, 2024, 28(5): 1699-1732.

Karthik, K. K., Cheriyan, B. V., Rajeshkumar, S., et al. A review on selenium nanoparticles and their biomedical applications. Biomedical Technology, 2024, 6: 61-74.

Lakowicz, J. R. Instrumentation for fluorescence spectroscopy, in Principles of Fluorescence Spectroscopy, edited by J. R. Lakowicz. Springer, Boston, pp. 27-61, 2006.

Liu, H., Cao, G. Effectiveness of the Young-Laplace equation at nanoscale. Scientific reports, 2016, 6(1): 23936.

Lv, P., Chang, Y., Liu, F., et al. CO_2-brine mass transfer patterns and interface dynamics under geological storage conditions. International Journal of Heat and Mass Transfer, 2024, 222: 125184.

Lv, P., Liu, Y., Yang, W. Investigation on CO_2 permeation in water-saturated porous media with disordered pore sizes. Experimental Thermal and Fluid Science, 2020, 119: 110207.

Maffei, M., Canova, D., Bertea, C. M., et al. UV-A effects on photomorphogenesis and essential-oil composition in Mentha piperita. Journal of Photochemistry and Photobiology B: Biology, 1999, 52(1-3): 105-110.

Mahendran, G., Rahman, L. U. Ethnomedicinal, phytochemical and pharmacological updates on peppermint (Mentha × piperita L.). Phytotherapy Research, 2020, 34(9): 2088-2139.

Martini, K. M., Boddu, S. S., Nemenman, I., et al. Maximum likelihood estimators for colony-forming units. Microbiology Spectrum, 2024, 12(9): e03946-23.

Mikhailova, E. O. Selenium nanoparticles: green synthesis and biomedical application. Molecules, 2023, 28(24): 8125.

Minakov, A. V., Pryazhnikov, M. I., Neverov, A. L., et al. Wettability, interfacial tension, and capillary imbibition of nanomaterial-modified cross-linked gels for hydraulic fracturing. Capillarity, 2024, 12(2): 27-40.

Nalawade, T. M., N., Bahat, K. G., Sogi, S. Antimicrobial activity of endodontic medicaments by agar well diffusion. International Journal of Clinical Pediatric Dentistry, 2016, 9(4): 335-341.

Oktay, M., Gülçin, I., Küfrevioğlu, Ö. I. Antioxidant activity of fennel seed extracts. LWT- Food Science and Technology, 2003, 36(2): 263-271.

Osman, H. H., Abdel-Hafez, H. F., Khidr, A. A. Efficacy of two nanoparticles and effective microorganisms on Spodoptera littoralis. International Journal of Agriculture Innovations and Research, 2015, 3(6): 1620-1626.

Park, H. E., Yang, S. O., Hyun, S. H., et al. Simple preparative gas chromatographic method for isolation of menthol and menthone from peppermint oil. Journal of Separation Science, 2012, 35(3): 416-423.

Peng, J., Zhang, L., Song, M., et al. NiFe hydroxide nanosheet synthesized by *in-situ* chelation for highly efficient oxygen evolution reaction. Materials Chemistry and Physics, 2021, 258: 123918.

Piacenza, E., Presentato, A., Heyne, B., et al. Tunable photoluminescence properties of selenium nanoparticles: Biogenic versus chemogenic synthesis. Nanophotonics, 2020, 9(11): 3615-3628.

Pisoschi, A. M., Pop, A., Georgescu, C., et al. Natural antimicrobials in food. European Journal of Medicinal Chemistry, 2018, 143: 922-935.

Purushothaman, G. Enumeration of twelve clinically important bacterial standards. International Journal of Creative Research Thoughts, 2018, 6(2): 880-893.

Raoof, G. F. A., El-anssary, A. A., Ali Abuaish, M. A., et al. Assessment of Vicia faba L. peels: Phytochemical characterization and evaluation of cytotoxic and antimicrobial potentials. Chemistry & Biodiversity, 2025, 22(2): e202402123.

Shahzadi, S., Fatima, S., Shafiq, Z., et al. A review on green synthesis of silver nanoparticles (SNPs) using plant extracts: a multifaceted approach in photocatalysis, environmental remediation, and biomedicine. RSC Advances, 2025, 15(5): 3858-3903.

Soni, M., Yadav, A., Maurya, A., et al. Advances in designing essential oil nanoformulations: An integrative approach to mathematical modeling with potential application in food preservation. Foods, 2023, 12(21): 4017.

Soundarya, V., Venkatesa Prabhu, S., Manivannan, S., et al. Biosynthesized AgNPs using Daphniphyllum neilgherrense. ChemistrySelect, 2025, 10(39): e02821.

Tharp, W. F., Abdul Karem, L. K., Karem, A., Chem, M. J. Green synthesis, characterization, antimicrobial and anticancer studies of zirconium oxide nanoparticles using thyme extract. Moroccan Journal of Chemistry, 2024, 12(2): 643-656.

Tharp, W. F., Karem, L. K. A. Preparation, diagnosis, theoretical study, biological evaluation and antioxidant assay of ZrO_2 nanoparticles by green method. Baghdad Science Journal, 2025, 22(11): 3610-3619.

Tran, P. A., Webster, T. J. Selenium nanoparticles inhibit Staphylococcus aureus. International Journal of Nanomedicine, 2011, 6: 1553-1558.

Turner, G. W., Gershenzon, J., Croteau, R. B. Development of peltate glandular trichomes of peppermint. Plant Physiology, 2000, 124(2): 665-680.

Xue, R., Chang, Y., Wang, S., et al. Pore-scale microfluidic investigation of unsaturated CO_2 bubble morphology and interface evolution during drainage-imbibition cycles. Capillarity, 2025, 15(3): 74-86.

Yarnell, E. Herbs for viral respiratory infections. Alternative and Complementary Therapies, 2018, 24(1): 35-43.

Zaidi, S., Dahiya, P. In vitro antimicrobial activity, phytochemical analysis and total phenolic content of essential oil from Mentha spicata and Mentha piperita. International Food Research Journal, 2015, 22(6): 2440-2445.

Zambonino, M. C., Quizhpe, E. M., Mouheb, L., et al. Biogenic selenium nanoparticles in biomedical sciences: Properties, current trends, novel opportunities and emerging challenges in theranostic nanomedicine. Nanomaterials, 2023, 13(3): 424.

Zarin, T., Aghajanzadeh, M., Riazi, M., et al. Experimental and numerical study of the water-in-oil emulsions in porous media. Capillarity, 2024, 13(1): 10-23.

Zhang, X., Liu, Z., Shen, W., et al. Silver nanoparticles: Synthesis, characterization, properties, applications, and therapeutic approaches. International Journal of Molecular Sciences, 2016, 17(9): 1534.